Zinc(II) complexes of 3–bromo–5–chloro–salicylaldehyde: Characterization and biological activity

Ariadni Zianna [a,*], Ellie Vradi,[b] Antonios G. Hatzidimitriou,[a] Stavros Kalogiannis,[b] George Psomas [a, *]

[a] *Laboratory of Inorganic Chemistry, Department of Chemistry, Aristotle University of Thessaloniki, Thessaloniki GR–54124, GREECE.*

[b] *Department of Nutritional Sciences and Dietetics, International Hellenic University, Sindos, Thessaloniki, GREECE.*

Supplementary information

[*] Corresponding authors e–mails:

ariadnezianna@gmail.com (A. Zianna); gepsomas@chem.auth.gr (G. Psomas)

S1 Interaction with CT DNA

The interaction of the compounds (3–Br–5–Cl–saloH and its complexes **1–5)** with CT DNA was investigated by UV–vis spectroscopy, viscosity measurements and fluorescence emission spectroscopy.

S1.1 Binding study with CT DNA by UV–vis spectroscopy

UV–vis spectroscopy was used for the evaluation of the interaction of the compounds with CT DNA, and specifically the possible binding modes of the compounds to CT DNA. Control experiments with DMSO were performed and no changes in the spectra of CT DNA were observed.

In order to determine the binding mode, the UV–vis spectra of the compounds were recorded for a constant concentration (10^{-4} M) with increasing concentrations of CT DNA for diverse *r* (*r* = [complex]/[DNA]) values. The changes of the absorbance of the UV–vis spectra were monitored and the DNA–binding constants (K_b, M^{-1}) of the compounds were calculated by the Wolfe–Shimer equation (eq. S1) [S1] and the plots [DNA]/(ε_A–ε_f) *versus* [DNA]:

$$\frac{[DNA]}{(\varepsilon_A - \varepsilon_f)} = \frac{[DNA]}{(\varepsilon_b - \varepsilon_f)} + \frac{1}{K_b(\varepsilon_b - \varepsilon_f)} \qquad \text{(eq. S1)}$$

where [DNA] = the concentration of DNA in base pairs, ε_f = the extinction coefficient for the free compound at the corresponding λ_{max}, $\varepsilon_A = A_{obsd}/[compound]$ and ε_b = the extinction coefficient for the compound in the fully bound form. K_b is given by the ratio of slope to the y intercept in plots [DNA]/(ε_A–ε_f) *versus* [DNA].

S1.2 CT DNA–binding studies by viscosity measurements

The viscosity of DNA (0.1 mM) in buffer solution was measured in the absence and presence of increasing amounts of the compounds. The experiments were executed at room temperature and the measurements are devised in a plot $(\eta/\eta_0)^{1/3}$ *versus* r, where η = the viscosity of DNA in the presence of the compound, and η_0 = the viscosity of DNA in buffer solution.

S1.3 EB–displacement studies

In order to determine and confirm the DNA–interaction mode of the compounds, a competitive study with EB as an intercalating marker was performed by fluorescence emission spectroscopy. Therefore, the EB–displacing ability of the compounds from its EB–DNA conjugate was examined.

The DNA–EB adduct was prepared by addition of 20 μM EB and 26 μM CT DNA in buffer solution (150 mM NaCl and 15 mM trisodium citrate at pH 7.0). The potential intercalation of the

compounds between the DNA–bases was studied by the addition of a certain amount of the compound solution into the EB–DNA adduct solution. The influence of the compounds on the EB–DNA solution was monitored through the changes of the fluorescence emission spectra at excitation wavelength (λ_{ex}) at 540 nm [S2]. The tested compounds do not show any significant fluorescence at room temperature in solution or in the presence of DNA, under the same experimental conditions (λ_{ex} = 540 nm). Bearing that in mind, the observed quenching of the EB–DNA solution is evidently associated to the displacement of EB from its EB–DNA adduct.

The quenching efficiency (K_{SV}) for each compound was assessed according to the Stern–Volmer equation (eq. S2) [S2]:

$$\frac{Io}{I} = 1 + k_q \tau_0 [Q] = 1 + K_{SV}[Q] \qquad \text{(eq. S2)}$$

where I_0 and I = the fluorescence emission intensities of EB–DNA in the absence and presence of the quencher, respectively, [Q] = the concentration of the quencher (i.e. compounds). K_{SV} is obtained from the Stern–Volmer plots by the slope of the diagram I_0/I *versus* [Q]. Taking τ_0 = 23 ns as the fluorescence lifetime of the EB–DNA system [S3], the EB–DNA quenching constants (k_q, in $M^{-1}s^{-1}$) of the compounds can be determined according to equation S3:

$$K_{SV} = k_q \tau_o \qquad \text{(eq. S3)}$$

S2 DNA–cleavage experiments

The reaction mixtures (20 μL) containing supercoiled circular pBR322 DNA stock solution (Form I, 50 μM/base pair, ~500 ng), compounds, and Tris buffer (25 μM, pH 6.8) in Pyrex vials were incubated for 30 min at 37 °C, and was centrifuged under aerobic conditions at room temperature.

After addition of the gel–loading buffer [6x Orange DNA Loading Dye 10 mM Tris–HCl (pH 7.6), 0.15% orange G, 0.03% xylene cyanol FF, 60% glycerol, and 60 mM EDTA, by Fermentas], the reaction mixtures were loaded on a 1% agarose gel with EB staining. The electrophoresis tank was attached to a power supply at a constant current (65 V for 1 h). The gel was visualized by 312 nm UV transilluminator and photographed by an FB−PBC−34 camera vilberlourmat. Quantification of DNA−cleaving activities was performed by integration of the optical density as a function of the band area using the program “Image J” available at the site http://rsb.info.nih.gov/ij/download.html.

The ss% and ds% damages were calculated according to the equations S4 and S5:

$$ss\% = \frac{FormII}{(FormI + FormII + FormIII)} \times 100 \qquad \text{(eq. S4)}$$

$$ds\% = \frac{FormIII}{(FormI + FormII + FormIII)} \times 100 \qquad \text{(eq. S5)}$$

where, as Form II we consider Form II of each series minus Form II of the irradiated control DNA and as Form I, we consider Form I of each series. The amount of supercoiled DNA was multiplied by factor of 1.43 to account for reduced EB intercalation into supercoiled DNA [S4].

S3 Interaction with serum albumins

The albumin–binding study for the compounds was carried out by fluorescence emission quenching experiments using BSA (3 μM) or HSA (3 μM) in buffer solution (15 mM trisodium citrate and 150 mM NaCl at pH 7.0). The tested compounds were used as quenchers with gradually increasing concentrations to monitor the quenching of the emission intensity of tryptophan residues of BSA at 345 nm or HSA at 340 nm [S2]. The fluorescence emission spectra were recorded between 300–500 nm with excitation wavelength of 295 nm. All the experiments were conducted at room temperature. The fluorescence spectra of the compounds were recorded under the same experimental conditions and presented a low–intensity emission band in the region 395–415 nm. Consequently, the SA fluorescence emission spectra were modified properly, by subtracting the spectra of the compounds, and quantitative studies followed.

The extent of the inner–filter effect can be roughly estimated with the following equation:

$$I_{corr} = I_{meas} \times 10^{\frac{\varepsilon(\lambda_{exc})cd}{2}} \times 10^{\frac{\varepsilon(\lambda_{em})cd}{2}} \qquad \text{(eq. S6)}$$

where I_{corr}= corrected intensity, I_{meas}= the measured intensity, c = the concentration of the quencher, d = the cuvette length (1 cm), $\varepsilon(\lambda_{exc})$ and $\varepsilon(\lambda_{em})$ = the ε of the quencher at the excitation and the emission wavelength, respectively, as calculated from the UV–vis spectra of the complexes [S5].

The interaction of the quencher (i.e. compounds) with serum albumins [S2] was studied through the Stern–Volmer and Scatchard equations [S2] and corresponding graphs. The values of the respective Stern–Volmer constant K_{SV} (M^{-1}), the quenching constant k_q ($M^{-1}s^{-1}$), the SA–binding constant K (M^{-1}) and the number of binding sites per albumin (n) were calculated.

According to Stern–Volmer quenching equation [S2] (eq. S2), where I_0 = the initial tryptophan fluorescence intensity of SA, I = the tryptophan fluorescence intensity of SA after the addition of the quencher, k_q = the quenching rate constants of SA, K_{SV} = the dynamic quenching constant, τ_0 = the average lifetime of SA without the quencher, [Q] = the concentration of the quencher), the Stern–Volmer constant (K_{SV}, M^{-1}) can be obtained by the slope of the diagram I_0/I *versus* [Q]. Taking $\tau_0 = 10^{-8}$ s as fluorescence lifetime of tryptophan in SA [S2], the quenching constant (k_q, $M^{-1}s^{-1}$) is calculated from equation S3.

From the Scatchard equation (eq. S7) [S2]:

$$\frac{\Delta I/I_0}{[Q]} = nK - K\frac{\Delta I}{I_0} \qquad \text{(eq. S7)}$$

where n = the number of binding sites per albumin and K = the SA–binding constant. The K constant (M^{-1}) is calculated from the slope in plots $(\Delta I/I_0)/[Q]$ *versus* $(\Delta I/I_0)$ and n is given by the ratio of y intercept to the slope [S6].

S4 Antioxidant biological assay

The antioxidant activity of the compounds was evaluated *via* their ability to scavenge *in vitro* free radicals such as DPPH and ABTS and to reduce H_2O_2. All the experiments were carried out at least in triplicate and the standard deviation of absorbance was less than 10% of the mean.

S4.1 Determination of the reducing activity of the stable radical DPPH

To an ethanolic solution of DPPH (0.1 mM) an equal volume solution of the compounds (0.1 mM) in ethanol was added. Absolute ethanol was also used as control solution. The absorbance at 517 nm was recorded at room temperature after 30 and 60 min, in order to examine the possible existence of a potential time–dependence of the DPPH radical scavenging activity [S8]. The DPPH–scavenging activity of the complexes was expressed as the percentage reduction of the absorbance values of the initial DPPH solution (DPPH%). NDGA and BHT were used as reference compounds.

S4.2 Assay of radical cation ABTS–scavenging activity

The ABTS assay was performed to determine the activity of compounds to scavenge the radical cation ABTS. Initially, a water solution of ABTS was prepared (2 mM). ABTS radical cation ($ABTS^{+\cdot}$) was produced by the reaction of ABTS stock solution with potassium persulfate (0.17 mM) and the mixture was stored in the dark at room temperature for 12–16 h before its use. The ABTS was oxidized incompletely because the stoichiometric reaction ratio of ABTS and potassium persulfate is 1:0.5. The absorbance became maximal and stable only after more than 6 h of reaction although the oxidation of the ABTS started immediately. The radical was stable in this form for more than 2 days when allowed to stand in the dark at room temperature. Afterwards, the $ABTS^{+\cdot}$ solution was diluted in ethanol to an absorbance of 0.70 at 734 nm and 10 μL of diluted compounds or standards (0.1 mM) in DMSO were added. The absorbance was recorded out exactly 1 min after initial mixing [S8]. The ABTS radical scavenging activity was expressed as the percentage inhibition of the absorbance of the initial ABTS solution (ABTS%). Trolox was used as an appropriate standard.

S4.3 Reduction of hydrogen peroxide

The ability of the compounds to reduce hydrogen peroxide was estimated according to the method described in the literature [S9]. The reaction mixture contained 20 μL of each of the test

compounds (0.1 mM) and 5 μL H_2O_2 solution (40 mM) in phosphate buffer (50 mM, pH 7.4). The absorbance was measured at 230 nm after 10 min. The antioxidant activity (reduction of hydrogen peroxide) of the compounds was expressed as the percentage decrease of the initial H_2O_2 solution (H_2O_2%). L–ascorbic acid (or vitamin C) was used as a standard.

S5 Antibacterial activity

The antimicrobial activity of the compounds was evaluated by determining their respective MIC values towards two Gram–(–) (*Escherichia coli* NCTC 29212 (*E. coli*) and *Xanthomonas campestris* ATCC 1395 (*X. campestris*)) and two Gram–(+) (*Staphylococcus aureus* ATCC 6538 (*S. aureus*) and *Bacillus subtilis* ATCC 6633 (*B. subtilis*)) bacterial species. Cultures of these microbial strains were grown on a rich selective agar medium and stored at 4°C. The selective media used were Nutrient Agar or Broth for *B. subtilis* and *S. aureus*, Yeast Mold Agar or Broth for *X. campestris* and Luria Agar or Broth for *E. coli*. Cells picked from the surface of the stored cultures were used to initiate liquid pre–cultures of the same selective medium at an initial turbidity of roughly 1 McFarland unit. Pre–cultures were incubated for 24 h in a rotary shaking incubator and subsequently they were used to inoculate the test cultures used for the determination of MIC at an initial turbidity of 0.5 McFarland units. The test cultures consisted of Mueller–Hinton broth (Deben Diagnostics Ltd) containing different concentrations of the compounds. Different concentrations were achieved as follows: the compounds were freshly dissolved in DMSO to a concentration of 1 mg mL^{-1} and they were diluted with DMSO, using the method of progressive double dilution. Therefore, working solutions with decreasing concentrations of the compounds under investigation were achieved. The working solutions were subsequently diluted to the final desired concentration by addition to the growth medium at a proportion of 2:98. MIC values were determined as the lowest concentrations of the tested compounds that inhibited visible growth of each respective organism after a 24 h incubation [S10]. Bacterial growth was determined by measuring the turbidity of appropriately diluted cultures at 600 nm with reference to equally diluted sterile growth medium and the inhibition achieved was calculated by comparing the turbidity of each culture to the average of the turbidity of three non–inhibited cultures. All test cultures were grown in triplicates and for the determination of MIC, growth had to be inhibited in at least two cultures of the triplicate. Incubation temperature at all stages was 37°C except for *X. campestris* that was cultivated at 28°C [S11].

S6 References

[S1] A. Wolfe, G. Shimer and T. Meehan, *Biochemistry*, 1987, **26**, 6392–6396.

[S2] J.R. Lakowicz, Principles of Fluorescence Spectroscopy, 3rd ed. Plenum Press, New York, 2006.

[S3] D.P. Heller and C.L. Greenstock, *Biophys. Chem*., 1994, **50**, 305–312.

[S4] A. Papastergiou, S. Perontsis, P. Gritzapis, A.E. Koumbis, M. Koffa, G. Psomas, K.C. Fylaktakidou, *Photochem. Photobiol. Sci.*, 2016, **15**, 351–360.

[S5] L. Stella, A.L. Capodilupo and M. Bietti, *Chem. Commun*., 2008, 4744–4746.

[S6] Y. Wang, H. Zhang, G. Zhang, W. Tao and S. Tang, *J. Lumin.*, 2007, **126,** 211–218.

[S7] N. Shahabadi, B. Bazvandi and A. Taherpour, *J. Coord. Chem*., 2017, **70**, 3186–3198.

[S8] C. Kontogiorgis and D. Hadjipavlou–Litina, *J. Enz. Inhib*. *Med. Chem*., 2003, **18,** 63–69.

[S9] R.J. Ruch, C. Cheng and J.E. Klaunig, *Carcinogenesis*, 1989, **10,** 1003–1008.

[S10] J.M. Andrews, *J. Antimicr*.*Chemotherapy*, 2001, **48**(S1), 5–16.

[S11] E.P. Irgi, G.D. Geromichalos, S. Balala, J. Kljun, S. Kalogiannis, A. Papadopoulos, I. Turel and G. Psomas, *RSC Adv*., 2015, **5**, 36353–36367.

Table S1. Crystallographic data, data collection and refinement details for complexes **1** and **3.**

	1	**3**
Crystal data		
Chemical formula	$C_{14}H_{10}Br_2Cl_2O_6Zn$	$C_{26}H_{14}Br_2Cl_2N_2O_4Zn$
M_r	570.32	714.50
Crystal system, space group	Monoclinic, $P2_1/c$	Orthorhombic, *Pbcn*
Temperature (K)	295	295
a (Å)	7.5788(7)	16.877(3)
b (Å)	27.462(3)	18.316(3)
c (Å)	8.6083(8)	8.1927(15)
β (°)	101.409 (4)	
V (Å^3)	1756.2 (3)	2532.5 (8)
Z	4	4
Radiation type	Mo *K*α	Mo *K*α
μ (mm^{-1})	6.28	4.37
Crystal size (mm)	0.19 × 0.14 × 0.12	0.18 × 0.17 × 0.14
Data collection		
Diffractometer	Bruker Kappa Apex2	
Absorption correction	Numerical	
	Analytical Absorption (De Meulenaer & Tompa, 1965)	
T_{min}, T_{max}	0.42, 0.47	0.48, 0.54
No. of measured, independent, observed [$I > 2.0\sigma(I)$] reflections	17110, 4020, 2768	14574, 2360, 1791
R_{int}	0.029	0.020
$(\sin\theta/\lambda)_{max}$ (Å^{-1})	0.650	0.611
Refinement		
$R[F^2 > 2\sigma(F^2)]$, $wR(F^2)$, *S*	0.033, 0.068, 1.00	0.036, 0.062, 1.00
No. of reflections	2768	1791
No. of parameters	226	168
H–atom treatment	H–atom parameters constrained	
$\Delta\rho_{max}$, $\Delta\rho_{min}$ (e Å^{-3})	1.12, −0.58	0.60, −0.59

Table S2. Hydrogen–bond geometry (Å, º) for complex **1**.

D*—H···*A	***D*—H (Å)**	**H···*A* (Å)**	***D*···*A* (Å)**	***D*—H···*A* (º)**
O5—H51···O4^{i}	0.81	2.20	2.896(7)	143
O5—H52···O2^{i}	0.82	2.09	2.761(7)	140
O6—H61···O2^{ii}	0.82	2.40	3.018(7)	134
O6—H62···O4^{ii}	0.82	1.98	2.732(7)	152

Symmetry codes: (i) −*x*+1, −*y*+1, −*z*+1; (ii) −*x*, −*y*+1, −*z*+1.

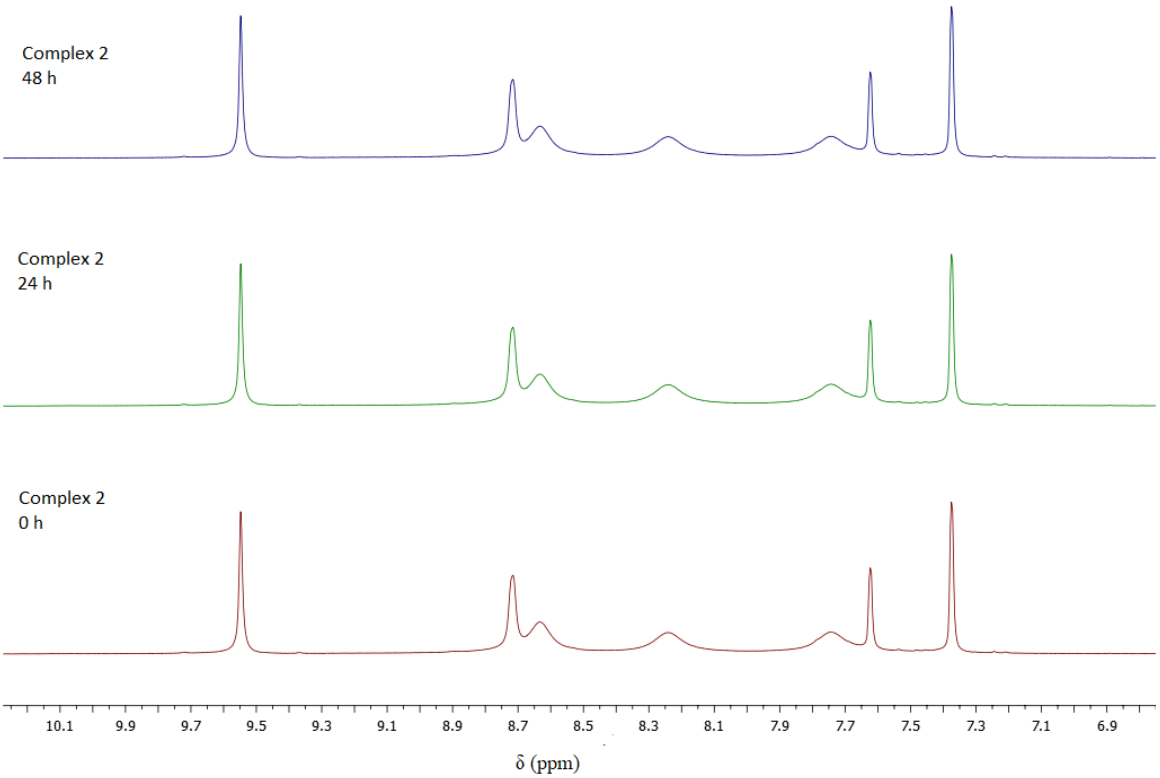

Figure S1. The ^{1}H NMR spectra of complex **2** in DMSO–d_6 at three different times (0, 24 h and 72 h).

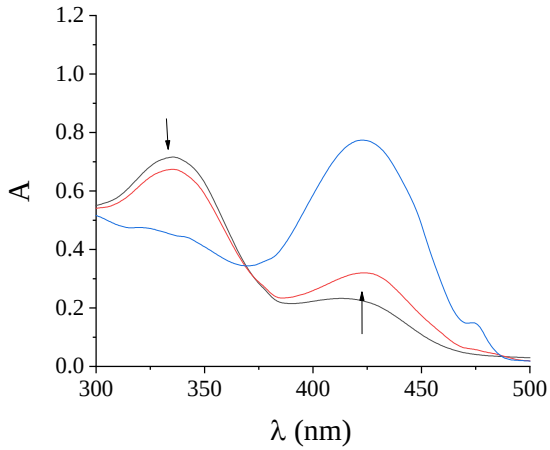

(A)

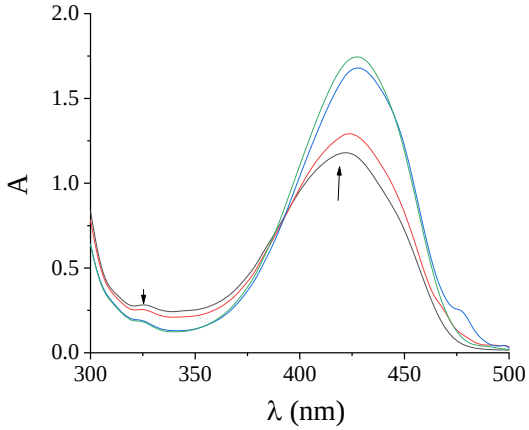

(B)

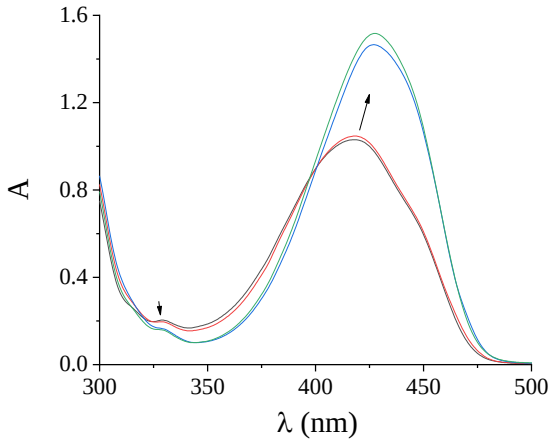

(C)

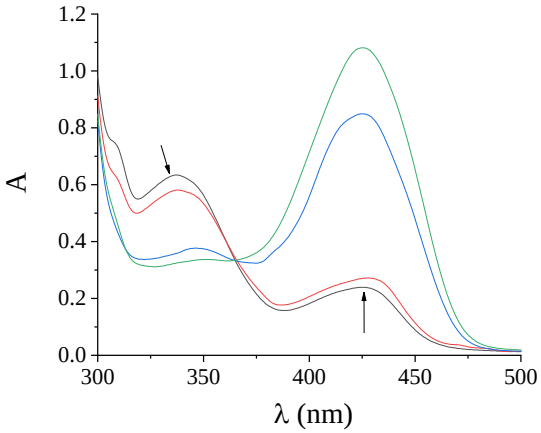

(D)

Figure S2. UV–vis spectra of DMSO solution (10^{-4} M) of complex (A) **1**, (B) **3**, (C) **4** and (D) **5** in the presence of increasing amounts of CT DNA. The arrows show the changes upon increasing amounts of CT DNA.

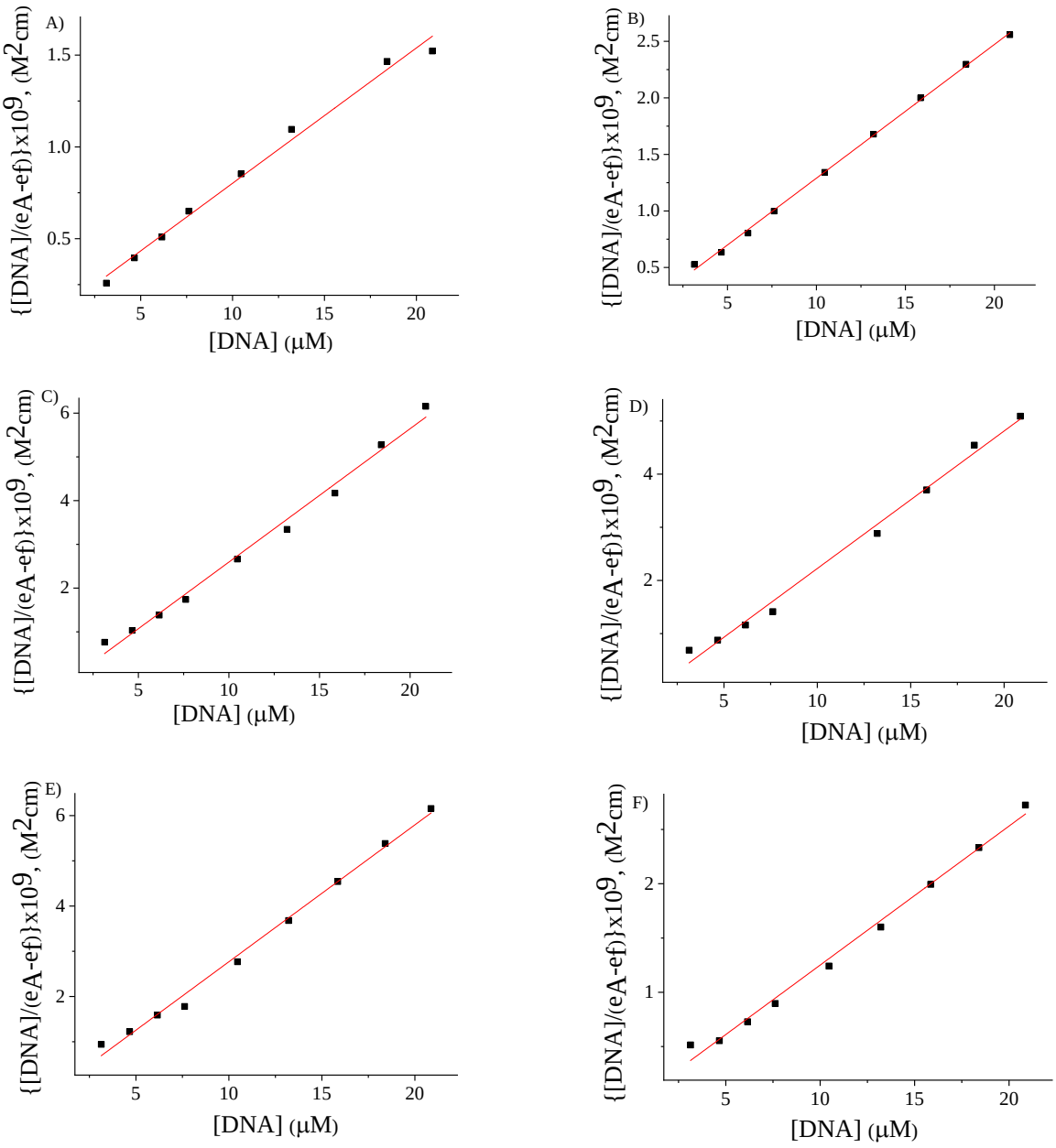

Figure S3. Plot of $\frac{[DNA]}{(\varepsilon_A - \varepsilon_f)}$ *versus* [DNA] for (A) 3–Br–5–Cl–saloH and (B–F) complexes **1–5.**

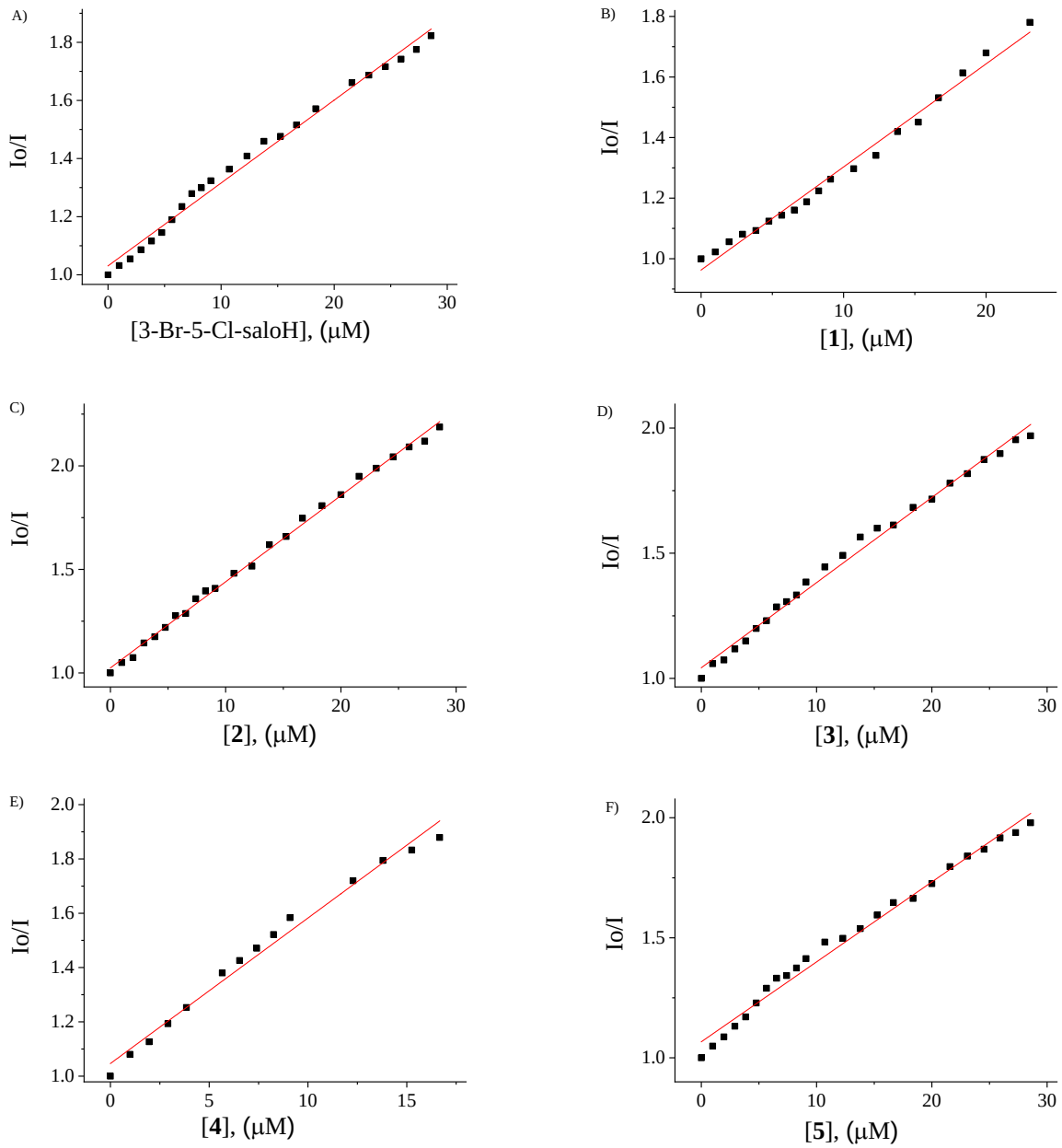

Figure S4. Stern–Volmer quenching plot of EB bound to CT DNA for (A) 3–Br–5–Cl–saloH and (B–F) complexes **1–5.**

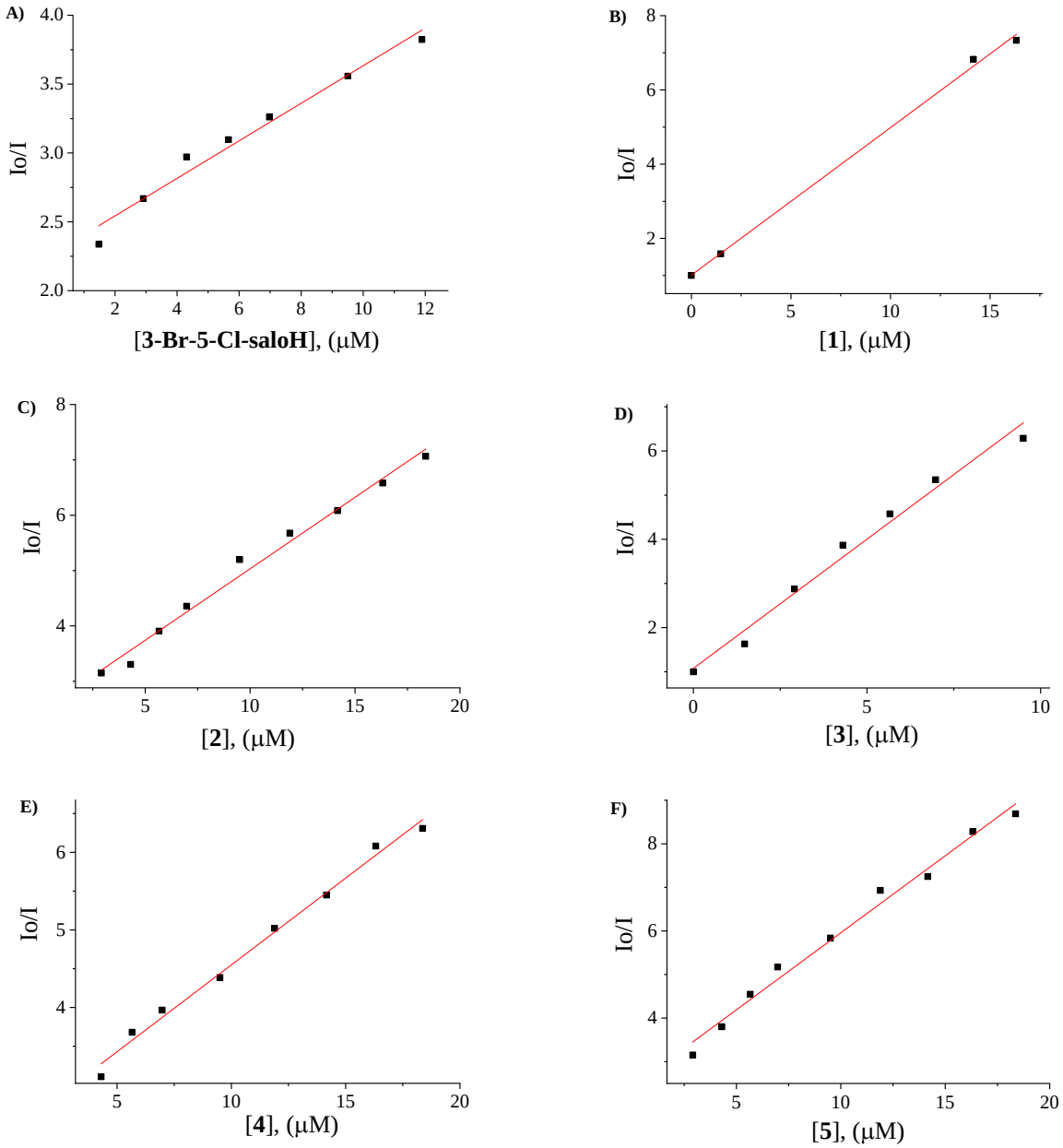

Figure S5. Stern–Volmer quenching plot of BSA for (A) 3–Br–5–Cl–saloH and (B–F) complexes **1–5.**

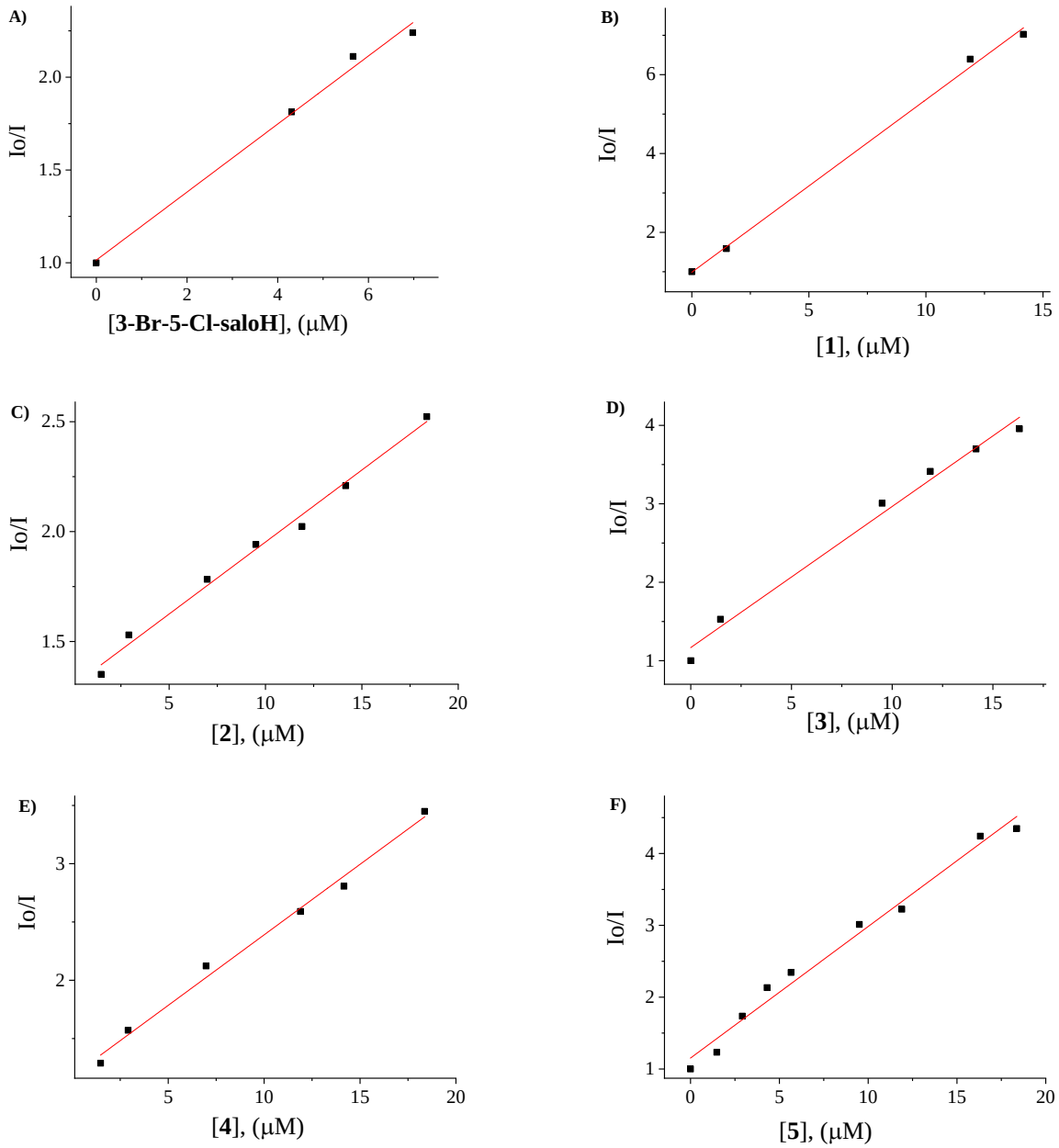

Figure S6. Stern–Volmer quenching plot of HSA for (A) 3–Br–5–Cl–saloH and (B–F) complexes **1–5.**

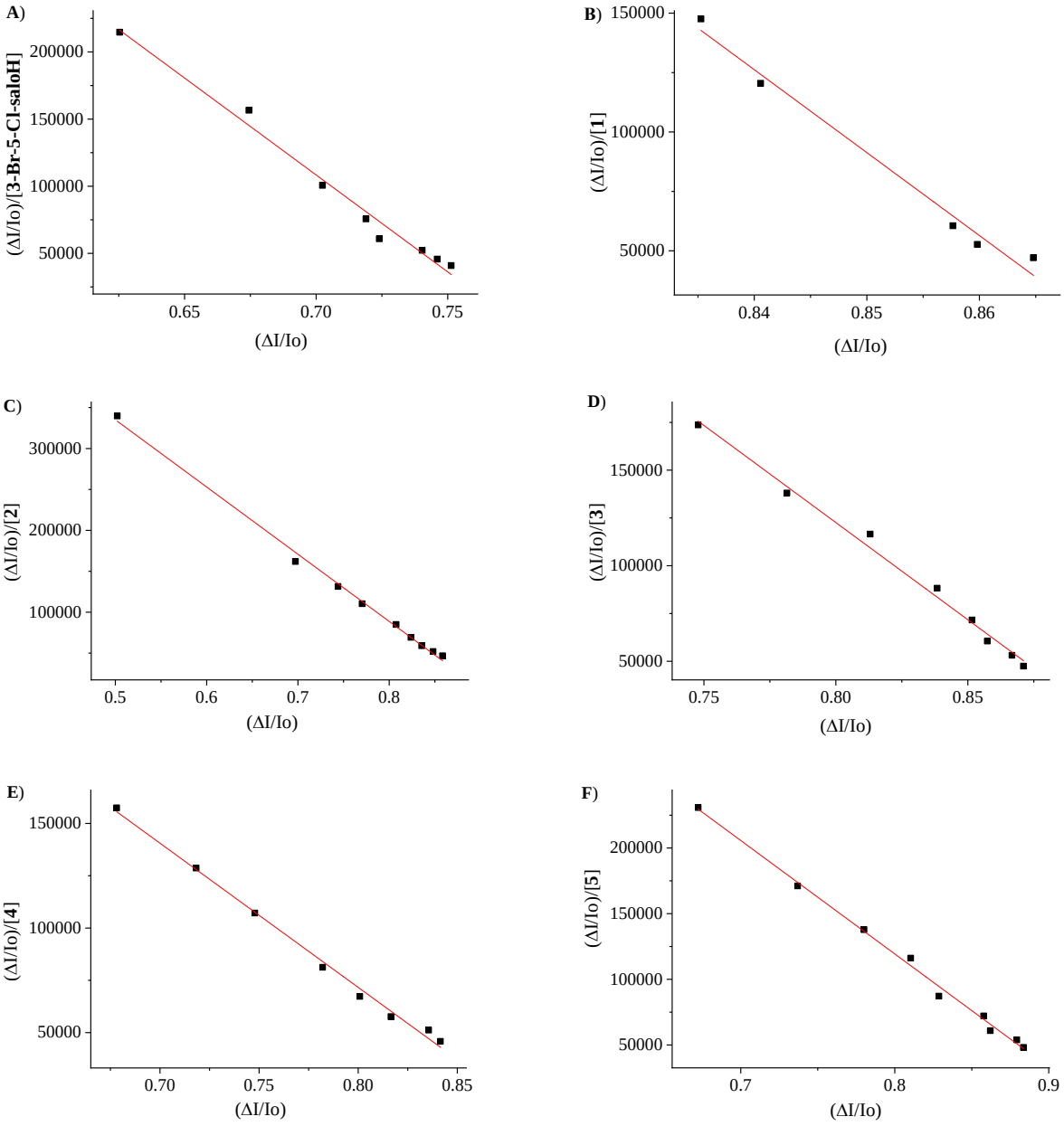

Figure S7. Scatchard plot of BSA for (A) 3–Br–5–Cl–saloH and (B–F) complexes **1–5.**

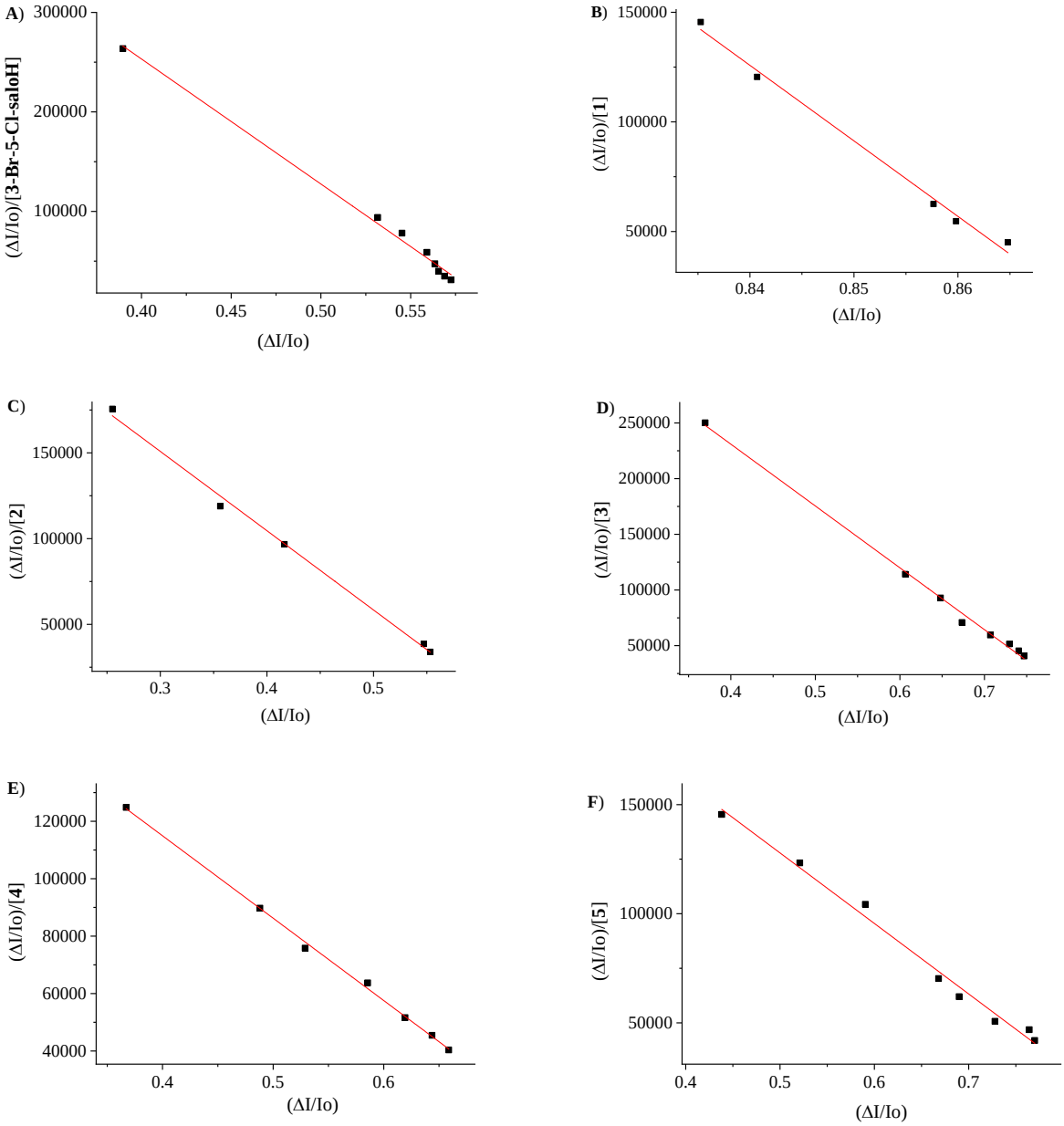

Figure S8. Scatchard plots of HSA for (A) 3–Br–5–Cl–saloH and (B–F) complexes **1–5.**